Dissolution experiments on dolerite quarry fines at low liquid-to-solid ratio: a source of calcium for MICP

Casas, Carla C.; Schaschke, Carl J.; Akunna, Joseph C.; Jorat, M. Ehsan

Published in:
Environmental Geotechnics

DOI:
10.1680/jenge.19.00067

Publication date:
2022

Document Version
Author accepted manuscript

Dissolution Experiments on Dolerite Quarry Fines at Low Liquid to Solid Ratio: A Source of Calcium for Microbial-Induced Calcite Precipitation

Author 1

- Carla C. Casas
- School of Applied Sciences, Division of Engineering and Food Science, Abertay University, Dundee, Scotland, United Kingdom.
- ORCID number: 0000-0003-0728-4395

Author 2

- Carl J. Schaschke
- School of Computing, Engineering and Physical Sciences, University of the West of Scotland, Paisley, Scotland, United Kingdom.
- ORCID number: 0000-0002-1655-7327

Author 3

- Joseph C. Akunna
- School of Applied Sciences, Division of Engineering and Food Science, Abertay University, Dundee, Scotland, United Kingdom.
- ORCID number: 0000-0002-6042-2809

Author 4

- M. Ehsan Jorat
- School of Applied Sciences, Division of Engineering and Food Science, Abertay University, Dundee, Scotland, United Kingdom.
- ORCID number: 0000-0001-6972-5921

Full contact details of corresponding author:

Carla Comadran Casas

Email: 1703065@uad.ac.uk

Tel: +34 607 39 10 07

Abstract (150 words)

Microbial Induced Calcite Precipitation (MICP) is an emerging soil stabilisation technique consisting of the precipitation of the mineral calcite in the soil matrix. Components required for MICP are currently industry end-products. In this paper, calcium release and reusability of calcium-rich silicate quarry fines, dolerite, are investigated in closed (batch reactor) and open (permeability test) systems at L/S ≤ 1.5 for MICP applications. The large specific surface area and reactive surface area accelerated calcium release, achieving calcium concentrations between 10 and 23 mM for different settings. Dissolution in batch reactor resulted in increased silt (<0.006 mm) and clay fractions. XRF analysis indicated no significant depletion of calcium in the dolerite after dissolution. The study shows dolerite quarry fines dissolution in distilled water at low L/S ratios is a rich source of calcium for MICP applications.

Keywords

Calcium carbonate; geomaterial characterisation; geochemistry

List of notations

λ	wavelength (nm)
ε_z	vertical strain (%)
ρ_s	particle density (Mg m^{-3})
ω_0	initial moisture (%)
D_i	particle diameter associated to the *i* percentage in a grain size distribution curve (mm)
C_u	coefficient of uniformity of the grain size distribution curve
C_c	coefficient of conformity of the grain size distribution curve
t	time (hours or seconds)
L/S	liquid to solid mass ratio (mL mg^{-1})
n	integer number
k	hydraulic conductivity (m s^{-1})
q	volumetric flow rate (m^3 s^{-1})
Δm	solute mass change due to weathering (mol)
R	weathering rate (mol m^{-2} s^{-1})
S	specific surface area (m^2 g^{-1})
S_0	specific unit area per unit volume of particles (m^2 m^{-3})
D_{eff}	effective particle diameter of the grain size distribution (cm)
SF	particle shape factor
Λ	surface roughness (m^2 m^{-2})

1. Introduction

There has been a steady shift in the conceptual understanding of soil as a living system, which has direct implications within civil engineering practice. Emerging bioremediations are increasingly based on soil stabilisation techniques over the traditionally known techniques such as grout injection (Dano et al., 2004), vibro/dynamic compaction (Gu and Lee, 2002) and installation of sand columns (Jorat et al., 2013). Among these, Microbial-Induced Calcite Precipitation (MICP) has proven successful in enhancing the mechanical properties of sands (DeJong et al., 2006; Montoya et al., 2013; Zamani and Montoya, 2015; Jiang and Soga, 2017; Zamani et al., 2018).

The technique relies on industrial products such as calcium chloride, urea and lab cultured strains. Alternative products to calcium chloride include seawater (Cheng et al., 2014); calcium lactate, calcium nitrate and calcium acetate (Zhang et al., 2014; Xu et al., 2015; Xu et al., 2015); egg shells (Choi Sun-Gyu et al., 2016); or limestone (Liu et al., 2017; Choi et al., 2017). To date, there has, however, been little attention to calcium-rich silicate rocks, which constitute a natural cementing agent through chemical weathering (DeJong et al., 2006) and, more specifically, to dolerite and basalt quarry fines (Manning, 2008).

The terms ‘quarry fines’ or ‘quarry dust’ are used in the mining sector for particle fractions smaller than 4 mm resulting from crushing, milling, scalping, dry sieving and washing aggregate processes in quarries. The ENV23 - UK statistics on waste (Fisher, 2014) estimate total annual quarry fines production to be 24.6 million tonnes. Currently, there is no specific market to consume its production (Mitchell et al., 2008) and recycling is environmentally disruptive and costly (Pilegis, 2014). This results in large stockpiles being accumulated in quarries (Mitchell et al., 2008), representing 99.2% of the total waste produced by the mining and quarrying sector. The latest report on UK mineral production (UKYM, 2015 by Idoine et al., 2016) estimate 43.7 million tonnes of aggregate production from igneous rocks in 2014 while the efficiency of the aggregate production process ranges between 3 to 40% (Mitchell et al., 2008). This accounts for production of between 1.3 and 17.5 million tonnes of igneous rocks quarry fines annually.

The rates at which mineral dissolution occurs depend on intrinsic factors such as mineral composition, weatherability, surface area, and extrinsic factors such as solute chemical composition, solute saturation state (Ω) and temperature (White and Buss, 2014). Chemical weathering increases in far-from-equilibrium (Ω <<< 1) conditions and higher temperatures, and the capacity of minerals to withstand chemical weathering (known as weatherability) decreases as the surface area increases. The weatherability of primary silicate minerals follows the order: olivine < pyroxene ~ amphibole < plagioclase < K-feldspar and the relative mobility of elements in silicate minerals, on a wt.% basis, follows Ca > Na > Mg > K = Mn > Si > Fe = Ti > Al (Eggleton et al., 1987). These factors stress the suitability of the fines-grained dolerite quarry fines to source for calcium via chemical weathering.

This article evaluates the suitability of dolerite quarry fines as a source of calcium by investigating the dolerite quarry fines' weatherability in open and closed systems, to provide a recommendation on its sustainable use with specific focus on MICP applications. A batch reactor was used to mix the quarry fines with water at various proportions and durations to identify optimum mixing time and mass ratio for maximum calcium concentration in the solution. The pH and concentration of dissolved elements of the solution were analysed. X-Ray Fluorescence was used to determine the initial and weathered chemical composition of the dolerite quarry fines. To replicate *in-situ* conditions, through gravitational flux, water was allowed to drain through a layer of dolerite quarry fines and effluent solute concentration in respect to time was measured.

2. Materials and methods

Dolerite quarry fines was sourced from Barrasford Quarry (Barrasford, Hexham NE48 4AP, operated by Tarmac Ltd) and oven-dried at 105-110ºC. The dry sieve method and hydrometer method were used to determine the material's particle size distribution (PSD) and the particle density of solids was determined by the gas jar method (BSI, 1990a), both in duplicate. X-Ray Fluorescence (XRF) bead fusion technique was used to determine the chemical composition of dolerite quarry fines and the ICP-OES and ICP-MS were used to determine the chemical composition of dissolved elements weathered from dolerite quarry fines in water samples. Batch reactor and permeability tests were used to induce weathering in closed and open systems, respectively.

2.1 Batch reactor experiments

A batch reactor was used to investigate calcium release from dolerite as a function of time, *t*, and mass of 'liquid' to 'solid' ratio (L/S) for MICP applications. Low L/S ratios were used to maximise calcium concentration in the solution. Distilled water was used to minimise the introduction of calcium carbonate. Dolerite quarry fines (25 g) and distilled water were placed in 250 mL beakers and stirred at 170 rpm on a rotatory plate (Shaking incubator 311DS; Labnet International Inc.) at controlled temperature of 25 ± 3ºC. Solution samples were obtained by gravitational filtration through filter paper (Whatman® qualitative filter paper, Grade 1). The solids remaining on the filter paper were air-dried and returned to the beaker. The procedure was repeated replacing the solution for new distilled water in consecutive days to assess the reusability of the material. To minimise the loss of solids, the same filter paper was used repeatedly, and the beaker sealed during the stirring to avoid evaporative loss of the solute. The first set of tests investigated the influence of time on chemical weathering by monitoring the calcium concentration at 2, 10 and 20 minutes and 1, 2, 8 and 24 hours at L/S = 1.0 after which the solution was replaced, and the procedure repeated in triplicate. Dolerite quarry fines at the end of this test was tested for PSD, particle density and XRF (wavelength-dispersive Panalytical PW2404 spectrometer; ISO 12677:2011; AMG Superalloys UK Ltd) to determine the physical and chemical changes induced by weathering. In addition, influence of mass ratio was investigated using L/S of 0.6-1.5 with L/S increments of 0.1 at a fixed stir time of two minutes to allow suitable interaction between the particles and the solution. The procedure was repeated in quadruplicate.

2.2 Permeability test

Permeability testing was used to reproduce field case-scenarios where the hydraulic gradient is dependent on the intrinsic properties of the material. This replicate *in-situ* condition where a layer of dolerite quarry fines is spread on a surface area to source calcium required for MICP treatment. A discontinuous flow approach was used to allow the solid-solute phases to reach near-to-equilibrium conditions by diffusion during resting intervals (equilibration time) and percolation of the calcium-enriched solution by advection during permeability tests. Dolerite quarry fines was placed into a permeability mould (permeameter) without compaction. The experiment sequence involved a saturation stage applying constant backpressure of 48 kPa for 24 hours followed by nine falling head permeability tests (ASTM, 2000). Equilibration time intervals in between permeability tests ranged

from 24 to 72 hours. No water head pressure was applied during equilibration time periods. Tap water was used for the tests according to the standards for permeability measurements. The calcium concentration of tap water was measured at 5 mg L^{-1} and considered negligible for the purposes of this study. The outlet solution was collected at regular intervals during the permeability tests for calcium quantification. In addition, an oedometric test (BSI, 1990b) on the dolerite quarry fines was conducted to determine the consolidation behaviour of the material during saturation at an induced backpressure of 48 kPa for 24 hours. The vertical linear strain in oedometric test was used to determine thickness of the specimen after saturation in the permeameter. The length of the specimen for each permeability test was calculated based on the difference between the specimen's length after saturation and the final measured specimen length, assuming a linear decrease during permeability tests.

2.3 Specific surface area and calcium weathering rate

The geometric specific surface area, S_{GEO} ($m^2\ g^{-1}$), of dolerite quarry fines was determined as the ratio of specific unit area per unit volume of particles, S_0 ($m^2\ m^{-3}$), and the particle density, $S_{GEO} = S_0/\rho_s$, where S_0 is the ratio between the particle shape factor, SF, and the effective diameter, D_{eff} (Carrier, 2003). A shape factor of 8.4 for angular shaped particles was used (Loudon, 1952) and D_{eff} was calculated from the PSD as:

$$D_{eff} = \left(\frac{100\%}{\sum [f_i / (D_{li}^{0.404} \times D_{si}^{0.595})]} \right) \quad (1)$$

where, f_i is the fraction of particles between two sieve sizes (or in its defect, particle diameter), in % and D_{li} and D_{si} are the larger and smaller sieve/particle diameter, respectively, in cm. Weathering rates in batch reactor were calculated using the BET specific surface area (S_{BET}) to account for the nonideal geometry of mineral surfaces. S_{BET} was calculated form S_{GEO} as $\Lambda = S_{BET}/S_{GEO}$ using a roughness factor, Λ, of 7.0 for unweathered silicate surfaces (White and Peterson, 1990). The weathering rate, R (mol $m^{-2}\ s^{-1}$) was calculated using:

$$R = \frac{\Delta m}{St} \quad (2)$$

where, Δm (mol) is the solute mass change, S ($m^2\ g^{-1}$) is the specific surface area and t (s) is the duration of the reaction.

2.4 Chemical analyses on solution samples

The chemical composition of dissolved elements Ca, Na, Mg, Mn, K, Al and Fe in water samples weathered from dolerite was determined by acidification followed by ICP-OES and ICP-MS (iCAP Thermo 6500; ISO 17025; i2 Analytical UK Ltd) analyses. The solution pH was determined using a pH meter (FiveEasy Mettler Toledo pH meter; probe LE409; uncertainty ±0.01) calibrated to 97% at two points (pH = 4.0 and 7.0).

Calcium concentration in solution samples were determined in triplicate by flame Atomic Absorption Spectroscopy (AAS, AAnalyst™ 200 Perkin Elmer Spectrometer) according to the method described in Fishman and Downs (1966). The linear range was characterised by $r^2 \geq 0.9990$; $SD_{max} = \pm 0.0031$ and $RSD_{max} < 0.8\%$ for $n = 3$. Standard checks were carried throughout ($SD_{max} = \pm 0.0118$, $RSD < 0.5\%$; $n = 3$). Where insufficient volume of sample was obtained for AAS analysis, calcium concentrations were determined in triplicate by titration employing Murexide as complexometric indicator. The dye working solution was prepared dissolving 10 mg of ammonium purpurate (Sigma-Aldrich Inc.) in 125 mL methanol (99.8% Anhydrous, Sigma-Aldrich Inc.), stirred overnight for complete dissolution and filtered. The stability of the filtered dye working solution was checked and confirmed to be stable for two working days. A pH = 13 buffer working solution was prepared by adding 1.5 mL of 8 M potassium hydroxide (KOH) solution to 50 mL distilled water. Preparation of the sample for scan consisted of adding 450 µL of buffer, 600 µL of dye and 20 µL of sample of unknown calcium concentration into 2 mL micro-centrifuge tubes (Fisherbrand) and centrifuging for two minutes at 5000 rpm (Microcentrifuge Espresso, Thermo Scientific UK Ltd.) to allow precipitation of magnesium as magnesium hydroxide. The aliquot was transferred into a cuvette (1.5 mL UV semi-micro disposable cuvettes; GMBH + CO KG, Wertheim, Germany) to determine the absorbance (DR5000 UV-VIS Spectrophotometer, Hach Lange Ltd) at $\lambda = 509$ nm. The calcium absorbance was a linear function of concentration within 0-25 mg L^{-1} range ($r^2 \geq 0.999$; $SD_{av} = \pm 0.051$; $RSD_{av} = 2.1\%$ for $n = 3$). Automatic pipettes BP 20-200 and BP 100-1000 µL (BioPette Labnet Int., Woodbridge, NJ, 07095, USA) with associated standard errors of ± 0.8 and ± 0.6-0.9%, respectively, were used thorough.

5. Results

5.1 Physical characterisation of dolerite quarry fines

The particle size distribution (PSD) of the quarry fines was found to be composed of >95% fine-grained particles with maximum particle size <0.212 mm (Table 1). Hydrometer results indicated the fines fraction distribution of 40% coarse silt, 32% medium silt, 13% fine silt and 10% clay. Based on the PSD, the coefficient of uniformity (C_u) and coefficient of curvature (C_c) (Table 1) the material classified as poorly graded fine-grained (ASTM, 2007). The initial moisture content (ω_0) of 1.3% was attributed to water spraying carried out in quarries to reduce dust particles suspension generated during crushing and milling processes. The particle density (ρ_s = 2.84 Mg m^{-3}) was found to be in accordance with reported literature for dolerite (Leaman, 1975; Sloane, 1991).

Table 1 Physical properties of the dolerite quarry fines.

Coarse (%) < 0.212 mm	Fines (%) < 0.063 mm	ρ_s (Mg m^{-3})	ω_0 (%)	D_{60} (mm)	D_{30} (mm)	D_{10} (mm)	C_u (-)	C_c (-)
4.88	95.12	2.84	1.3	0.025	0.009	0.002	12.5	1.6

In the oedometric test, a vertical pressure of 47.6 kPa induced a vertical strain ($\Delta\varepsilon_z$) of 15.9%. The total vertical strain induced during permeability test sequence (saturation, permeability tests and equilibration time periods) was 18.3%. Accordingly, consolidation occurred mainly during the saturation stage. The vertical strain during permeability tests occurred due to rearrangement of particles under the influence of hydraulic flow. The average permeability (± one standard deviation) of the nine tests was found equal to 2.62x10^{-7} (± 9.18·10^{-8}) m s^{-1}.

5.2 Dissolved elements from dolerite quarry fines in water

Table 2 presents the chemical composition of dissolved elements weathered from dolerite quarry fines in three water samples determined by ICP-OES and ICP-MS analyses. Analysed samples were

obtained from batch reactor experiments for L/S = 1.0 at different stir times (*t*) and number of solution replacements (*n*) indicated in Table 2. The concentration of dissolved elements consistently followed the order Ca > Na > Mg > Mn > K > Al > Fe which is agreement with reported literature (Polynov, 1937; Asio and Jahn, 2007). The highest concentrations and largest decrease in solute concentration with number of water replacements were observed for Ca and Na.

Table 2 ICP-OES and ICP-MS Analyses. Concentration of dissolved elements in water solution weathered from dolerite quarry fines. Solution samples were obtained by gravitational filtration after stir times *t* (h) and *n* water replacements at L/S = 1.0 in batch reactor. Units in mg L^{-1}.

no.	*t* (h)	*n*	Ca	Na	Mg	Mn	K	Al	Fe
1	1	2	420	150	38	23	12	0.028	0.010
2	2	2	380	130	35	15	12	0.022	0.013
3	8	3	120	48	8.6	6.5	6.1	0.061	0.017

5.3 Calcium concentration as a function of time in batch reactor and permeability tests

The evolution of the solute calcium concentration as a function of time for L/S = 1.0 in batch reactor is presented in Figure 1 in which three water replacements are identified by *n* = 1, 2 and 3 trends. Three stages were identified. At the far-from-equilibrium initial stage (S1), the calcium concentration in the solution increased rapidly up to one hour and equilibrium between the solid and liquid phases was attained between one to two hours. The calcium concentrations at 2, 10 and 20 minutes were the same attributed to having similar liquid-solid phase contact times during the filtration process. A steady state (S2) was identified between two and eight hours. In the third stage (S3), calcium concentration in the solution decreased between eight and 24 hours. With respect to calcium levels at eight hours, a decrease of -2.1 (<10%), -1.4 (< 10%) and -4.9 mM (58%) in calcium concentration occurred for *n* = 1, 2 and 3, respectively.

Calcium concentrations after two hours of stirring resulted in solute calcium concentrations for *n* = 1, 2 and 3 of 23, 15 and 9 mM, respectively, which indicated the reusability of the material of at least three times.

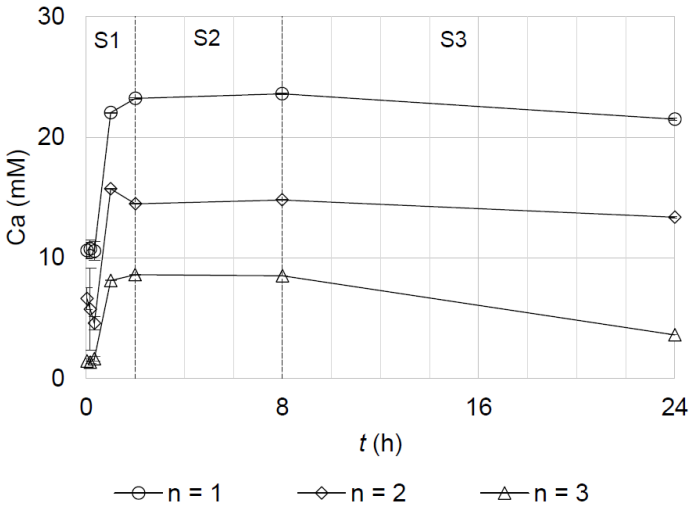

Figure 1 Concentration of calcium weathered from dolerite in water samples as a function of time at constant volume, temperature (25 ± 3ºC) and solid-solute mass ratio (L/S = 1.0) in batch reactor setting. Trends *n* = {1, 2, 3} are discrete values of solute concentration of repeated tests on reused material obtained by gravitational filtration and new water additions. Markers and vertical error bars are computed average and standard deviation of three measurements.

The solute calcium concentration monitored during permeability tests sequence presented in Figure 2 indicated the reusability of the material for at least five water discharges where the percolated water contained calcium concentrations ranging from 8 to 17 mM. A convex parabolic relationship was found between the number of water discharges and the solute calcium concentration after the second water discharge. A decrease in the solute calcium concentration was observed during each water discharge between second and fourth water discharges however, this was not observed for the first water discharge. As the number of water discharge increased the variation in calcium concentration reduced. The duration of the tests during the initial five permeability tests increased from 12 to 20 minutes during which a continuous flow of calcium-enriched solution poured out of the dolerite quarry fines layer at an average volumetric flux of 5.01×10^{-5} $m^3 s^{-1}$ per square metre.

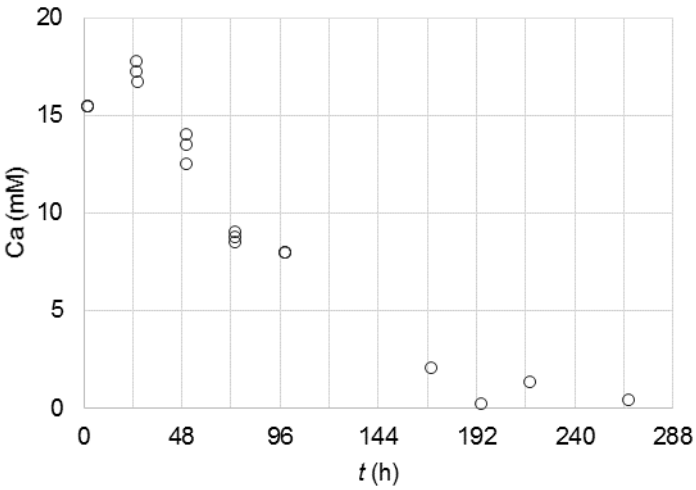

Figure 2 Calcium concentration evolution in outlet solution samples over a 12-day period and nine permeability tests. Horizontal axis is organised as the chronological sequence of permeability tests (grouped markers) and equilibration time intervals ranging from 24 to 72 hours. Markers indicate specific sampling times. Saturation time prior the initial test was of 24 hours at 48 kPa backpressure.

5.3.1 pH evolution as a function of time in batch reactor

In general, higher pH values of the filtered solutions were measured with increased number of water replacements (Figure 3). The largest increase in pH occurred at far-from-equilibrium conditions (S1) which corresponded to the largest release of calcium in Figure 1. Once the system approached near-to-equilibrium conditions (t > 1 hour) pH followed different trends for n = 1, 2, 3. At n = 1, pH increased up to one hour and remained steady (pH = 7.3) until the end of the test. At n = 2, pH peaked at two hours (pH = 7.8) and decreased up to 24 hours. At n = 3, pH peaked (pH = 8.0) at eight hours followed by a gentle drop between 8 to 24 hours.

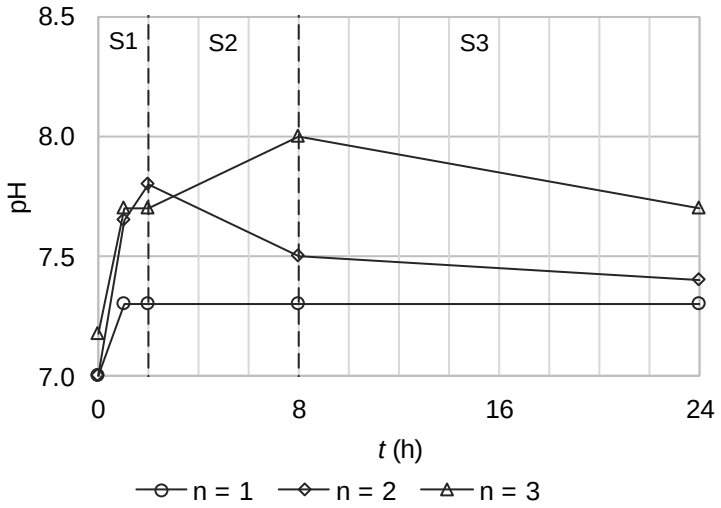

Figure 3 pH evolution as a function of time in solution samples during batch reactor experiments for L/S = 1.0 and three water replacements.

5.3.2 Physicochemical changes induced by dissolution in batch reactor

Dissolution of dolerite quarry fines in batch reactor for L/S = 1.0 and *n* = 3 induced an increase in the particle density from 2.84 to 2.91 Mg m^{-3}. Sedimentation by hydrometer tests on the material prior (UW) and after (W) dissolution (Figure 4) showed a larger percentage of fine silt (<0.006 mm) and clay size fractions whereas the medium and coarse silt fraction remained unaltered. The particle effective diameter (Eq. 1.) increased slightly (0.0969 to 0.1005 mm) and the BET surface area decreased from 0.214 to 0.201 m^2 g^{-1} as a result of the increase in particle density.

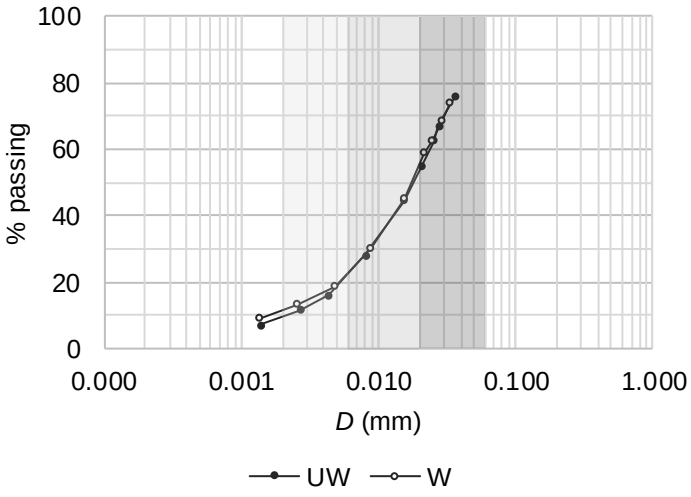

Figure 4 Effect of chemical weathering on fines content grain size distribution. Sedimentation by hydrometer test of dolerite quarry fines samples prior and after dissolution in batch reactor. Results are in duplicate. The weathered sample was obtained after 24 hours of stirring and three solution replacements at L/S = 1.0 in batch reactor.

The XRF analysis (Table 3) revealed the chemical composition of the material used in this study (U and W) and the dolerite (ND) described in Randall (1989), both sourced from Barrasford, are practically identical indicating the analyses are comparable. The main differences are slightly less silicate and aluminium and magnesium oxide contents against slightly increased content of iron, titanium and calcium oxides, respectively. Further, the water and inorganic carbon content are higher in the sample used in this study.

The XRF analysis of the material prior and after dissolution (Table 3) showed no significant change in the chemical composition of the material occurred as a result of the dissolution experiment, the only exception being an enrichment of titanium oxides. Calcium mass balance, calculated as the ratio of cumulative mass of calcium measured in water samples (Figure 1) to the equivalent mass of calcium in the rock (Ca = 9.37 wt. %) calculated from XRF data, indicated 2% of the total mass of calcium contained in the rock was released during the dissolution experiment between one to eight hours. Based on the XRF data and the chemical composition of dissolved elements in water samples in Table 2, the order of loss of elements based on the total element composition of dolerite prior to dissolution on a wt.% basis followed Ca > Na > Mg > K > Mn > Fe > Al which is in good agreement with Polynov's series and reported literature (Polynov, 1937; Goldich, 1938; Tiller, 1958; Eggleton et al., 1987).

Table 3 Chemical composition of this study's dolerite quarry fines (U and W) determined by XRF and Randall (1989)'s dolerite from Barrasford (ND) determined using wet-chemical methods. Dolerite quarry fines prior (U) and after (W) dissolution in batch reactor for 24 hours and three water replacements at L/S = 1.0. 3*SD* column indicate the analytical precision of the XRF technique as three standard deviation. ND sample is identified as ND WS-1 in Table 11 of Randall (1989). Fe_2O_3 and

Mn_2O_3 values in ND column correspond to the sum of FeO and Fe_2O_3 and to MnO in Randall (1989), respectively. Units in wt. %.

Element	3*SD*	UW	W	ND
SiO_2	±0.42	47.72	47.73	49.85
Al_2O_3	±0.21	13.49	13.39	14.02
Fe_2O_3	±0.21	12.95	13.09	12.56
CaO	±0.20	10.34	10.18	9.33
MgO	±0.14	5.2	5.21	6.01
TiO_2	±0.09	2.46	2.61	2.28
Na_2O	±0.09	2.44	2.37	2.42
K_2O	±0.06	0.95	0.95	0.93
P_2O_5	±0.05	0.42	0.41	0.28
Mn_3O_4	±0.03	0.18	0.19	0.18
LOI	±0.11	3.57	3.17	1.31
Total	±0.60	99.82	99.46	99.34

5.3.3 Calcium weathering rate in batch reactor

Calcium weathering rates based on changes in solute concentration were calculated for S1 in Figure 1 where calcium concentration increased as a function of time. The average calcium weathering rates (Eq. 2) after one hour of stirring were 2.95×10^{-8} ($\pm 1.22 \times 10^{-10}$) mol m^{-2} s^{-1}, 2.11×10^{-8} ($\pm 8.69 \times 10^{-10}$) mol m^{-2} s^{-1} and 1.09×10^{-8} ($\pm 4.49 \times 10^{-10}$) mol m^{-2} s^{-1} for n = 1, 2 and 3, respectively. Values in between parenthesis correspond to ±1 standard deviation.

5.4 Calcium concentration as a function of liquid to solid mass ratio in batch reactor

The effect of varying the 'liquid' to 'solid' mass ratio (L/S) on solute calcium concentration and reusability of the solid phase is presented in Figure 5. For L/S > 1.0, larger volume of liquid with respect to solid allowed for a larger initial release of calcium for n = 1, effect that was not satisfied with subsequent water replacements (n = 2 and 3). The calcium concentration at L/S = 1.5 for n = 1 after two minutes of stirring was 17 mM compared to the 11 mM achieved at L/S = 1. This may indicate a

lower reusability of the solid or longer stir times however, further measurements are required to confirm it. For L/S < 1.0, both the solute concentration and reusability increased, although less solution volume was obtained. For L/S = 0.8, the solute calcium concentration raised above 20 mM and was maintained for *n* = 2. Further water replacement (*n* = 3 and 4) indicated the reusability of the material of at least four times at L/S < 1.0, although L/S < 0.7 were not suitable as most of the solution was retained in the solid phase.

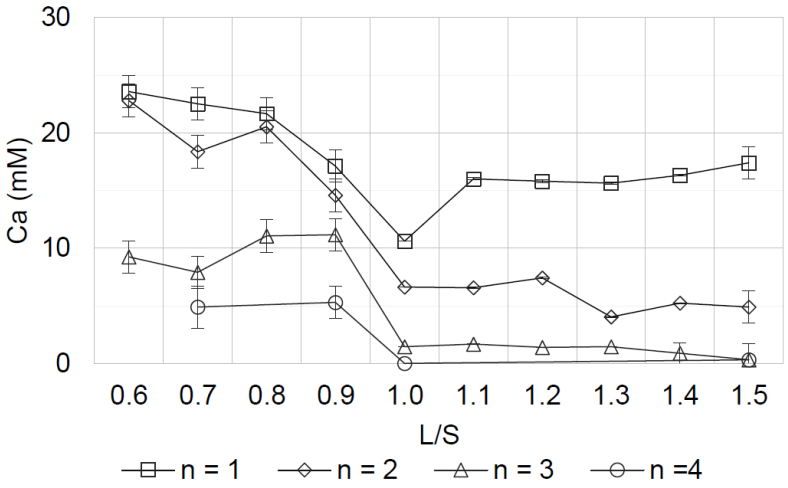

Figure 5 Liquid to solid mass ratio influence on solute calcium concentration in water samples obtained from batch reactor experiments at constant volume, temperature (25 ± 3ºC) and residence time of two minutes. Trends *n* = {1, 2, 3 and 4} are discrete values of solute calcium concentration of repeated tests on reused material obtained by gravitational filtration and new water additions. Markers and vertical error bars are computed average and standard deviation of three measurements.

6. Discussion

6.1 Material characterisation

McClelland's (1949) study on the influence of time, temperature and particle size distribution on weathering rates indicate that the rate at which elements in a primary mineral are released into solution approach in time the ratio in which these elements are present in the parent mineral. Subsequent studies (Creasey et al., 1986; Yoshioka, 1987) related the chemical composition of stream water to the parent rock mineral composition. In this study, because Ca and Na are released at a fast rate, the largest concentration of Ca relative to Na in solution indicated the major mineral

constituents of dolerite quarry fines sourced from Barrasford were composed of calcium-rich silicate minerals.

The chemical composition of quarry fines determined by XRF analysis had nearly the same composition to that determined by wet-chemical methods for dolerite (Table 3) in Randall (1989). In particular for dolerite, the feldspar phase is composed mostly of plagioclase ($An_{64\text{-}68}Ab_{30.5\text{-}35.5}Or_{0.5\text{-}1.5}$), containing between 1.1-2.6 wt.% of FeO; the pyroxene phase consist of pigeonite ($Wo_{8\text{-}9}En_{62\text{-}66}Fs_{26\text{-}29}$), calcium-rich pyroxene lying within the augite field ($Wo_{37}En_{46}Fs_{17}$) and orthopyroxene ($Wo_5En_{66}Fs_{29}$); calcic amphiboles; and iron-titanium oxides (ilmenite-ulvospinel) which underwent oxidation exsolution and further altered to mainly sphene, and potentially to pseudobrookite or rutile.

The chemical composition of this material, along with the large surface area (S_{BET} = 0.212 $m^2\,g^{-1}$) resulting from the crushing and milling processes indicated the suitability of dolerite quarry fines to source calcium at a fast rate required for MICP.

The observed increase in particle density after dissolution in batch reactor experiments was related to the precipitation of high-density secondary minerals product of the weathering of silicate rocks, in particular oxide minerals. Iron oxides, such as maghemite (5.49 Mg m^{-3}), hematite (5.30 Mg m^{-3}), magnetite (5.15 Mg m^{-3}) or goethite (4.27 Mg m^{-3}); titanium oxides, such as rutile (4.25 Mg m^{-3}) and anatase (3.88 Mg m^{-3}) are denser than parent minerals, e.g. anorthite (2.75 Mg m^{-3}) or wollastonite (2.91 Mg m^{-3}).

6.2. Rate of calcium release

Dissolution experiments of crystalline basalt at ambient temperature, circumneutral pH and distilled water in batch reactor were carried out by Gislason and Eugster (1987). However, experiments were conducted far-from-equilibrium at L/S = 50 and 100 for up to four months. In this study, the release of calcium occurred at a fast rate until steady state was achieved between one to two hours.

Calcium weathering rates within this initial phase were found several orders of magnitude greater than those reported in Gislason and Eugster (1987) attributed to the measurement time span difference. Reported weathering rates of basalts and silicate minerals in the literature (Bandstra et al., 2008) are based on silica release instead of calcium and do not allow direct comparison.

In the batch reactor experiments, repeated enhancement of calcium release with solution replacement was attributed to the far-from-equilibrium initial conditions inducing a sharp increase of etch pit formation on mineral surfaces (Teng, 2004). Lower calcium concentrations with increased number of solution replacements indicated the influence of far-from-equilibrium initial conditions decreased as weathering advanced presumably due to a decreased overall reactive surface area. XRF results showing no significant variation in chemical composition induced by dissolution indicated the fast calcium release observed during batch reactor experiments was related mainly to the large reactive surfaces originated by the physical breakdown of the parent material during crushing and milling processes, which led to the large initial release of calcium.

For the permeability tests sequence equilibration times of 24 hours were found insufficient to achieve equilibrium between the second and fourth water discharge leading to a decrease in solute concentration during advection flow. This was not observed for the first and fifth discharges. This presents a complex relationship between the equilibration time requirement and weathering by diffusion. This is thought to be due to the large reactive surface area of the unweathered material leading to a rapid initial release of calcium, reducing the necessary equilibration time below 24 hours for the first water discharge. As the reactive surface area decreased and lower concentrations were required to achieve equilibrium, 24 hours were sufficient while, in between, larger equilibration times were necessary.

6.3 Calcium and pH evolution as a function of time

In the batch reactor experiments, the pH increased in time far-from-equilibrium coinciding with the largest release of calcium and larger pH values were found with increased number of solution replacements. Weathering by the action of water occurs through replacement of cations of the primary silicate mineral surface by dissociated hydrogen atoms from water molecules and the release of these cations causes the solute pH to rise (Jenny, 1950). As chemical weathering advances the surface area increases and hydrogen atoms penetrate further into the mineral structure resulting in larger pH increase.

Once the system reached equilibrium pH followed different trends and calcium concentration and pH drops were consistently observed between eight and 24 hours. Reaction of atmospheric carbon dioxide with water molecules in alkaline solutions and precipitation of calcite during weathering

(Gislason and Eugster, 1987; Stockmann, G. et al., 2008) could explain the pH and calcium drops. Indeed, calcite precipitation in soils associated with dolerite dissolution occurring as a natural phenomenon, known as inorganic passive carbon sequestration, was demonstrated in Manning et al. (2013). The pH and calcium concentration drops, however, occurring at different time intervals suggest other mechanisms may be involved.

6.4 Considerations regarding MICP

Calcium chloride concentrations ranging from 50 to 250 mM have been typically used for MICP studies however, lower concentration of 10 mM (Cheng et al., 2014) have been proved successful in inducing calcite precipitation although the necessary number of treatments (200) increased substantially. Liu, Liu et al. (2017) and Choi, Chu et al. (2017) dissolved quarry limestone using an acid solution to source calcium for MICP however, the use of an acid required of readjustment of pH to circumneutral prior to inducing MICP and the loss of carbon dioxide during the limestone dissolution process. In this study, calcium concentrations in solution above 20 mM were achieved for L/S = 1.0 in the batch reactor for a minimum stir time of one to two hours. For L/S = 1.5 stir time was reduced to 2 minutes achieving calcium concentration of 17 mM and larger volume of calcium-enriched solution. Similarly, for L/S = 0.8 (t = 2 min) calcium concentration in the solution raised above 20 mM for at least two water replacements. For the permeability test sequence, equilibration times of 24 hours were sufficient to maintain calcium concentrations above 10 mM for three water discharges. In any case, alkaline pH of the calcium-enriched solution was readily compatible with calcite precipitation. In addition, the presence of divalent cations such as Mg and Fe which form carbonate minerals (magnesite and siderite, respectively) increase the potential of carbonate precipitation.

Conclusions

The rate of calcium release from dolerite quarry fines and pH evolution was investigated in a closed batch reactor at L/S = 1.0 and three solution replacements. Calcium equilibrium between the liquid and solid phases was attained between one to two hours and removal of calcium from the solution occurred from eight to 24 hours. Both phenomena occurred systematically with increased number of solution replacements. Increase of the fine silt and clay size fractions occurred as a result of

dissolution whereas the medium and coarse silt fractions remained unaltered. Post-equilibrium pH and calcium concentration drops indicate atmospheric inorganic carbon may have entered the solution leading to the precipitation of calcite. Total calcium release was a direct function of time up to equilibrium and was maximised if calcium reached equilibrium prior to replacing the calcium-enriched solution. Further experiments are required to confirm this is satisfied for variable mass ratios and determine the equilibrium time points for maximum calcium release.

Calcium concentrations compatible with MICP treatments were obtained while dissolution in batch reactor induced no significant change in the chemical composition of the material. This highlights the relevance of the large reactive surface area originated from quarry crushing and milling processes and the potential of dolerite quarry fines dissolution for applications requiring of alkaline calcium-enriched solutions, such as MICP or inorganic carbon sequestration via carbonate precipitation.

Acknowledgements

This work was carried out with financial support of the Norman Fraser Design Trust, the Scottish Alliance for Geoscience, Environment and Society (SAGES) and RLINCS program of Abertay University for which the authors are thankful. Special thanks for the support by the laboratory technicians of Abertay University, R. Campbell and L. Milne, and the manager of Barrasford quarry, S. Bell, for sourcing the material used in this study.

References

Asio V and Jahn R (2007) Weathering of basaltic rock and clay mineral formation in Leyte, Philippines. Philippine Agricultural Scientist **90(3)**: 192-204.

ASTM (2017) D2487. Standard Practice for Classification of Soils for Engineering Purposes (Unified Soil Classification System). ASTM International.

ASTM (2000) D5084. Standard Test Methods for Measurement of Hydraulic Conductivity of Saturated Porous Materials Using a Flexible Wall Permeameter. ASTM International.

Bandstra JZ, Buss HL, Campen RK et al. (2008) Appendix: Compilation of mineral dissolution rates. In *Kinetics of Water-Rock Interaction* (Brantley SL, White AF and Kubicki JD (eds)). Springer Science+Business Media, LLC, New York, pp. 737-823.

BSI (1990a) 1377-2. Methods of test for soils for civil engineering purposes. Classification tests. BSI.

BSI (1990b) 1377-5. Methods of test for soils for civil engineering purposes. Compressibility, permeability and durability tests. BSI.

Carrier WD (2003) Goodbye, Hazen; Hello, Kozeny-Carman. Journal of Geotechnical and Geoenvironmental Engineering **129(11)**: 1054-1056.

Cheng L, Shanin MA and Cord-Ruwisch R (2014) Bio-cementation of sandy soil using microbially induced carbonate precipitation for marine environments. Géotechnique **64(12)**: 1010-1013.

Choi Sun-Gyu, Shifan W and Jian C (2016) Biocementation for Sand Using an Eggshell as Calcium Source. Journal of Geotechnical and Geoenvironmental Engineering **142(10)**: 0601-6010.

Choi SG, Chu J, Brown RC, Wang K and Wen Z (2017) Sustainable Biocement Production via Microbially Induced Calcium Carbonate Precipitation: Use of Limestone and Acetic Acid Derived from Pyrolysis of Lignocellulosic Biomass. ACS Sustainable Chemistry & Engineering **5(6)**: 5183-5190.

Creasey J, Edwards AC, Reid JM et al. (1986) The use of catchment studies for assessing chemical weathering rates in two contrasting upland areas in northeast Scotland. In *Rates of chemical weathering of rocks and minerals* (Colman S and Dethier D (eds)). Academic Press, Orlando, pp. 467-502.

Dano C, Hicher P and Tailliez S (2004) Engineering properties of grouted sands. Journal of Geotechnical and Geoenvironmental Engineering **130(3)**: 328-338.

DeJong JT, Fritzges MB and Nusslein K (2006) Microbial induced cementation to control sand response to undrained shear. Journal of Geotechnical and Geoenvironmental Engineering **132(11)**: 1381-1392.

Eggleton RA, Foudoulis C and Varkevisser D (1987) Weathering of basalt: changes in rock chemistry and mineralogy. Clays and Clay Minerals **35(3)**: 161-169.

Fisher K (2014) ENV23 - UK statistics on waste. Department for Environment, Food & Rural Affairs, https://www.gov.uk/, Report last updated 9 October 2018.

Fishman MJ and Downs SC (1966) Methods for analysis of selected metals in water by atomic absorption. USGPO, Washington, USA, Report 1540-C, pp. 26-28.

Gislason SR and Eugster HP (1987) Meteoric water-basalt interactions. I: A laboratory study. Geochimica et Cosmochimica Acta **51(10)**: 2827-2840.

Goldich SS (1938) A Study in Rock-Weathering. The Journal of geology **46(1)**: 17-58.

Gu Q and Lee F (2002) Ground response to dynamic compaction of dry sand. Géotechnique **52(7)**: 481-493.

Idoine NE, Bide T, Brown TJ and Raycraft ER (2016) United Kingdom Minerals Yearbook 2015. British Geological Survey, Keyworth, Nottingham, Report Open report, OR/16021.

Jenny H (1950) Origin of soils. In *Applied sedimentation* (Trask P (ed)). John Wiley and Sons, New York, pp. 41-61.

Jiang N- and Soga K (2017) The applicability of microbially induced calcite precipitation (MICP) for internal erosion control in gravel–sand mixtures. Géotechnique **67(1)**: 42-55.

Jorat ME, Kreiter S, Moerz T, Moon V and de Lange W (2013) Strength and compressibility characteristics of peat stabilized with sand columns. Journal of Geomechanics and Engineering **5(6)**: 575-594.

Leaman DE (1975) Form, mechanism, and control of dolerite intrusion near Hobart, Tasmania. Journal of the Geological Society of Australia **22(2)**: 175-186.

Liu L, Liu H, Xiao Y et al. (2017) Biocementation of calcareous sand using soluble calcium derived from calcareous sand. Bulletin of Engineering Geology and the Environment **77**: 1781-1791.

Loudon AG (1952) The Computation of Permeability from Simple Soil Tests. Géotechnique **3(4)**: 165-183.

Manning DAC (2008) Biological enhancement of soil carbonate precipitation: passive removal of atmospheric CO2. Mineralogical Magazine **72(2)**: 639-649.

Manning DAC, Renforth P, Lopez-Capel E, Robertson S and Ghazireh N (2013) Carbonate precipitation in artificial soils produced from basaltic quarry fines and composts: An opportunity for passive carbon sequestration. International Journal of Greenhouse Gas Control **17**: 309-317.

McClelland JE (1949) The effect of time, temperature and particle size on the release of bases from some common soil-forming minerals of different crystal structure.

Mitchell CJ, Mitchell P and Pascoe RD (2008) Quarry fines minimisation: can we really have 10mm aggregate with no fines? In *Proceedings of the 14th Extractive industry geology conference* (Geoffrey Walton (ed)). EIG Conferences, pp. 37-44.

Montoya BM, DeJong JT and Boulanger RW (2013) Dynamic response of liquefiable sand improved by microbial-induced calcite precipitation. Géotechnique **63(4)**: 302-312.

Pilegis M (2014) Structural and geo-environmental applications of waste quarry dust.

Polynov BB (1937) *The Cycle of Weathering*. T. Murby, London.

Randall BAO (1989) Dolerite-pegmatites from the Whin Sill near Barrasford, Northumberland. Proceedings of the Yorkshire Geological Society **47(3)**: 249-265.

Sloane DJ (1991) Some physical properties of dolerite. Division of Mines and Mineral Resources, Tasmania Department of Resources and Energy, Report 1991/22.

Stockmann G, Wolff-Boenisch D, Gislason S and Oelkers E (2008) Dissolution of diopside and basaltic glass: the effect of carbonate coating. Mineralogical Magazine **72(1)**: 135-139.

Teng HH (2004) Controls by saturation state on etch pit formation during calcite dissolution. Geochimica et Cosmochimica Acta **68(2)**: 253-262.

Tiller KG (1958) The geochemistry of basaltic materials and Australia associated soils of south-eastern south Australia. Journal of Soil Science **9(2)**: 225-241.

White A,F. and Buss H,L. (2014) Natural Weathering Rates of Silicate Minerals. In *Treatise on Geochemistry* (Holland DH and Turekian KK (eds)). Elsevier, Amsterdam.

White AF and Peterson ML (1990) Role of Reactive-Surface-Area Characterization in Geochemical Kinetic Models. In *Chemical Modeling of Aqueous Systems II* (Daniel C, Melchior R and Bassett L (eds)). American Chemical Society, vol. 416, pp. 461-475.

Xu J, Du Y, Jiang Z and She A (2015) Effects of calcium source on biochemical properties of microbial CaCO3 precipitation. Frontiers in Microbiology **6**: 1366.

Yoshioka R (1987) Geochemical study of weathering through chemical composition in natural waters. The Journal of Earth Sciences, Nagoya University **35(2)**: 417-444.

Zamani A., Feng K. and Montoya BM (2018) Improved Liquefaction Resistance from Microbial Induced Carbonate Cementation. In *Geotechnical Earthquake Engineering and Soil Dynamics V: Liquefaction Triggering, Consequences, and Mitigation* (Brandenberg SJ and Manzari MT (eds)). American Society of Civil Engineers, Online, pp. 296-303.

Zamani A and Montoya B (2015) Undrained Behavior of Silty Soil Improved with Microbial Induced Cementation. In *Proceeding of the 6th International Conference on Earthquake Geotechnical Engineering* (Anonymous). International Society for Soil Mechanics and Geotechnical Engineering, Online.

Zhang Y, Guo HX and Cheng XH (2014) Influences of calcium sources on microbially induced carbonate precipitation in porous media. Materials Research Innovations **18**: 79-84.

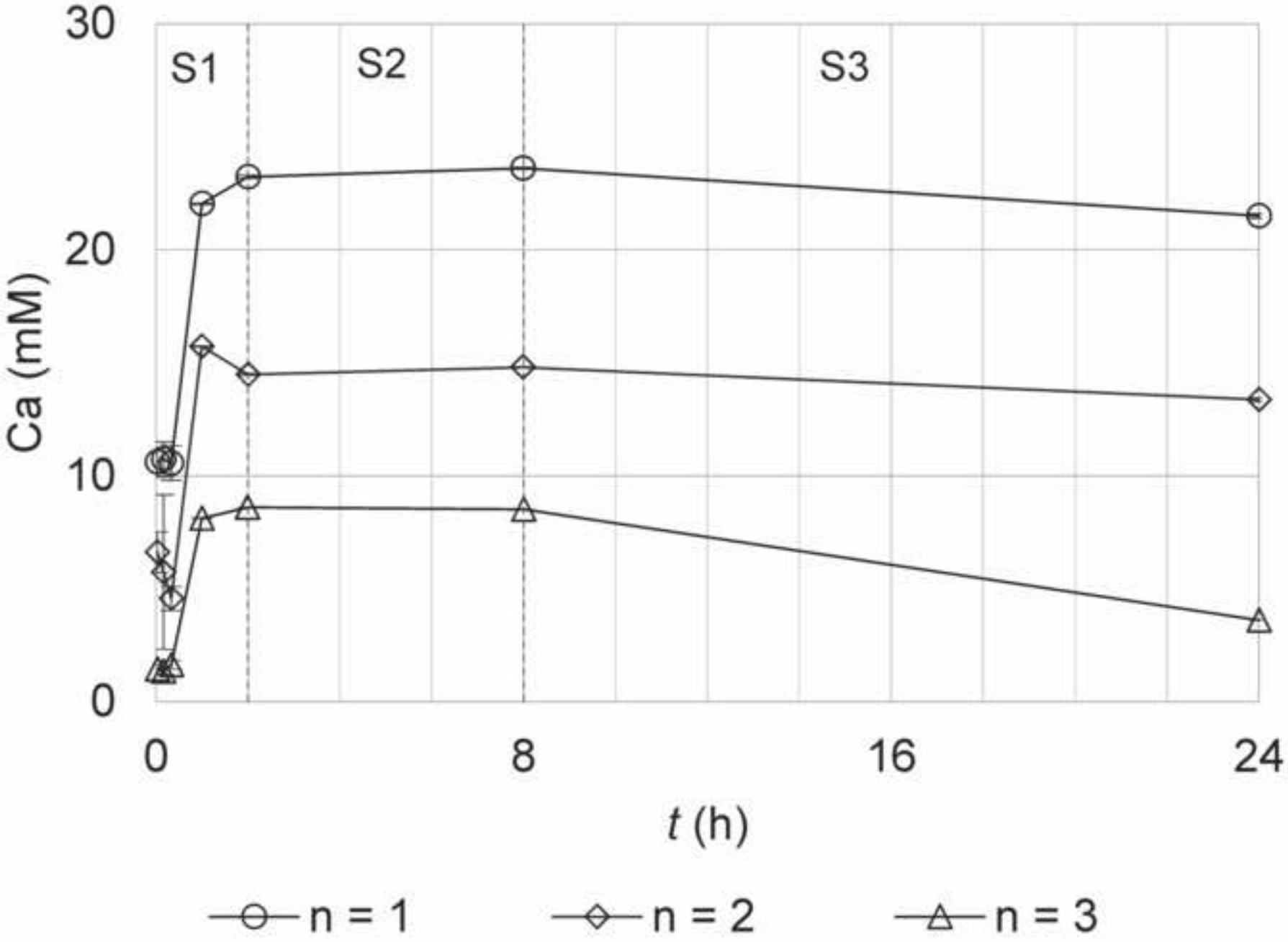

Figure2

Click here to access/download;Figure;Figure 2.tif

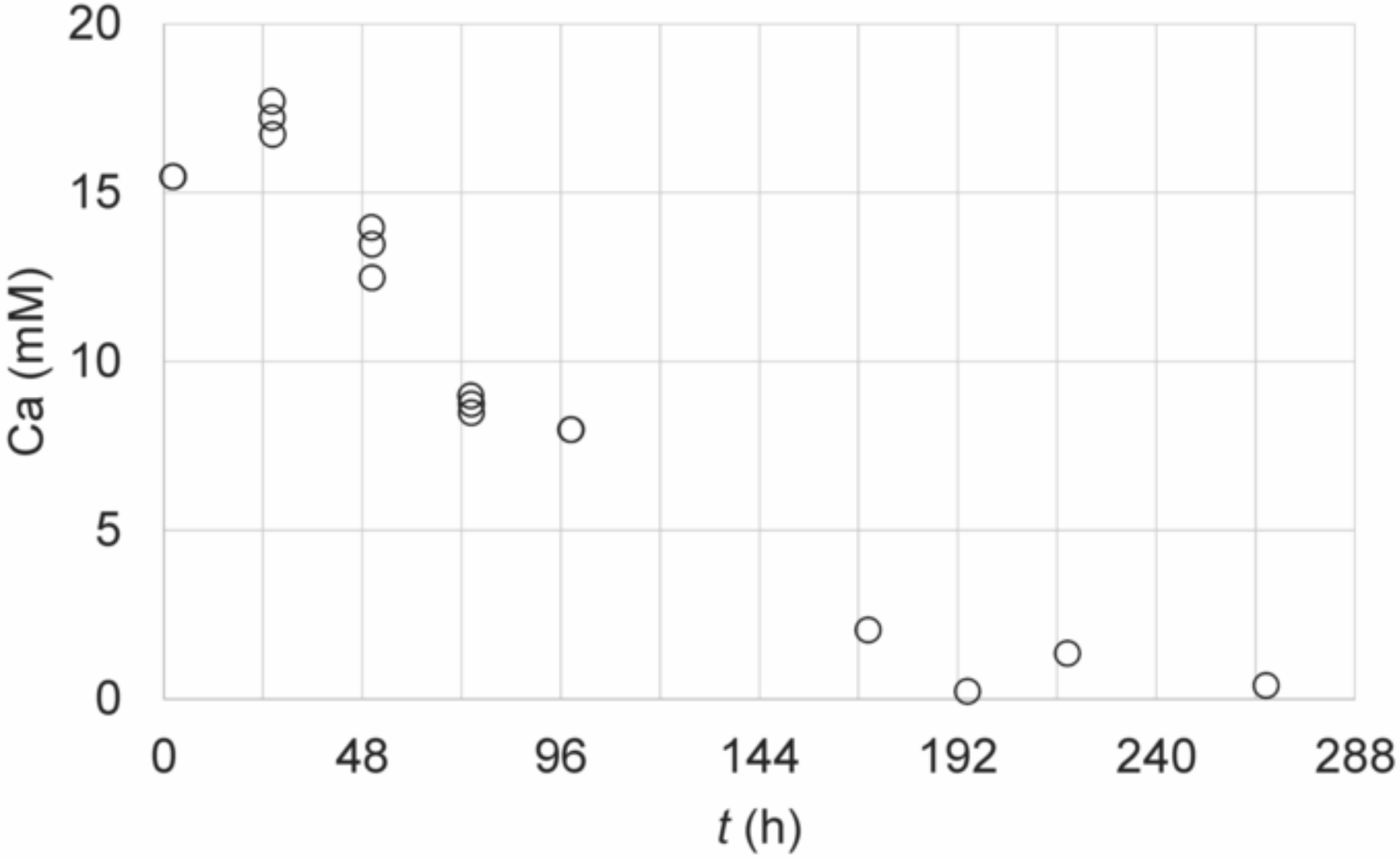

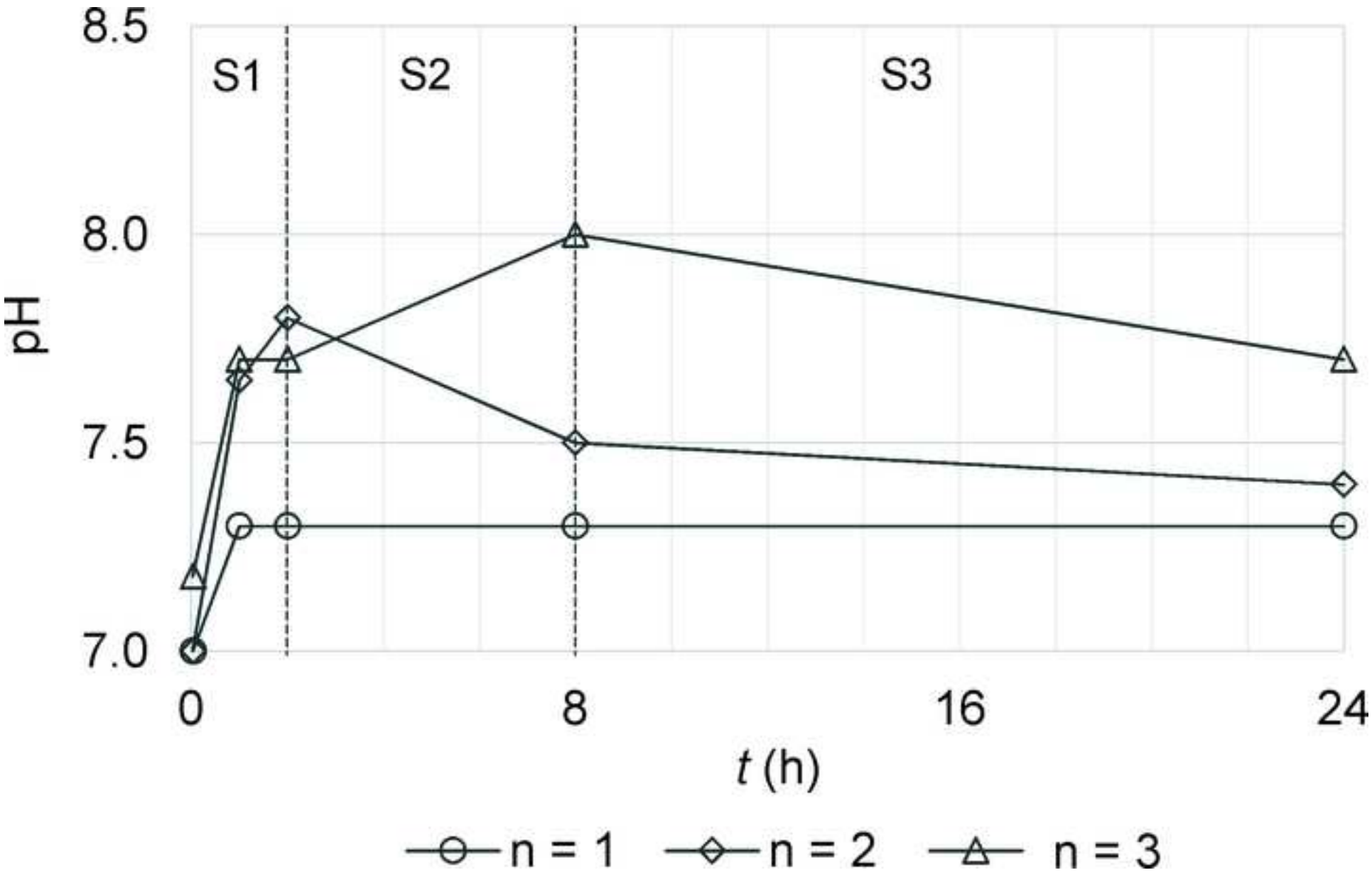

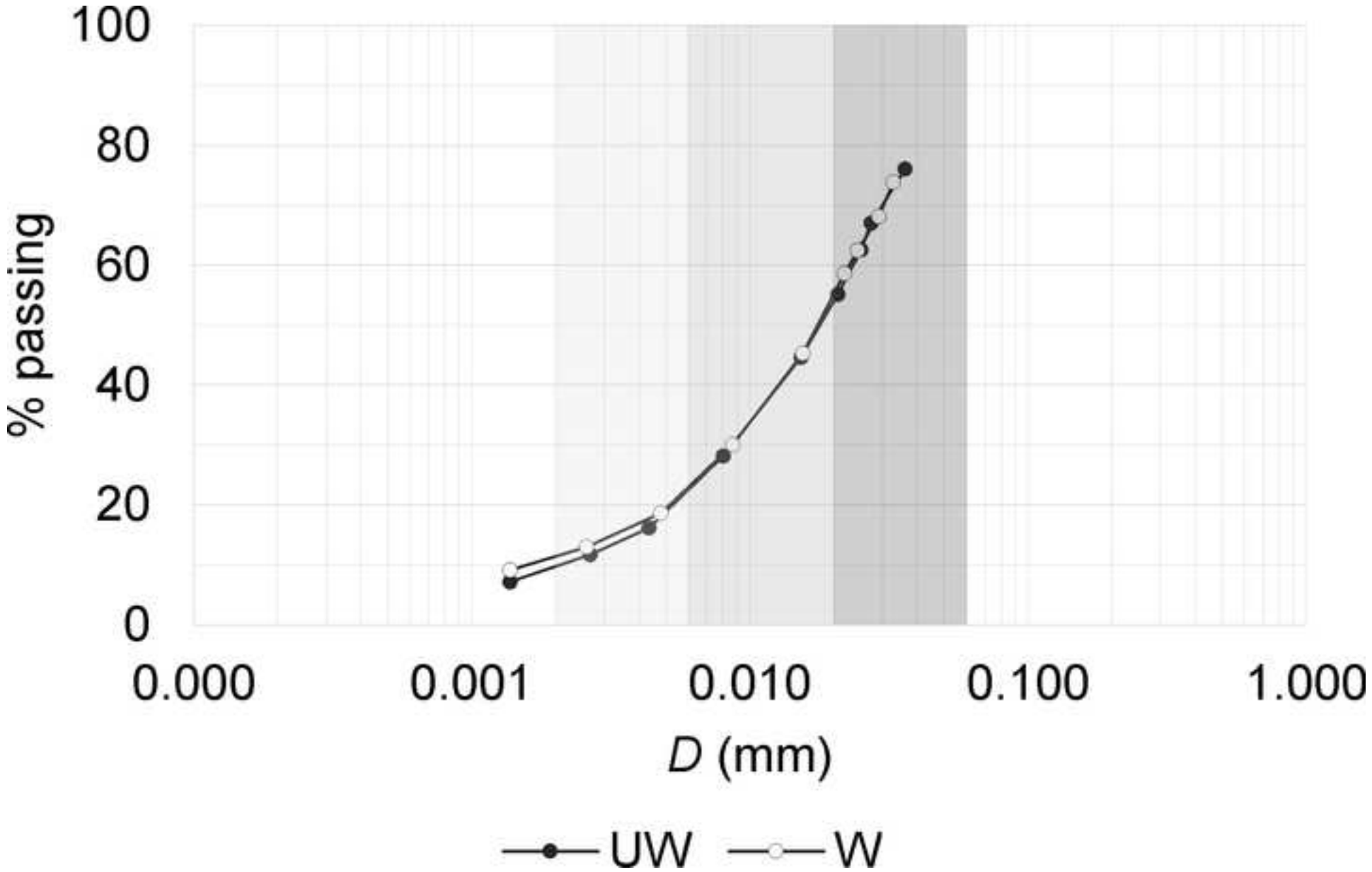

Figure5

Click here to access/download;Figure;Figure 5.tif

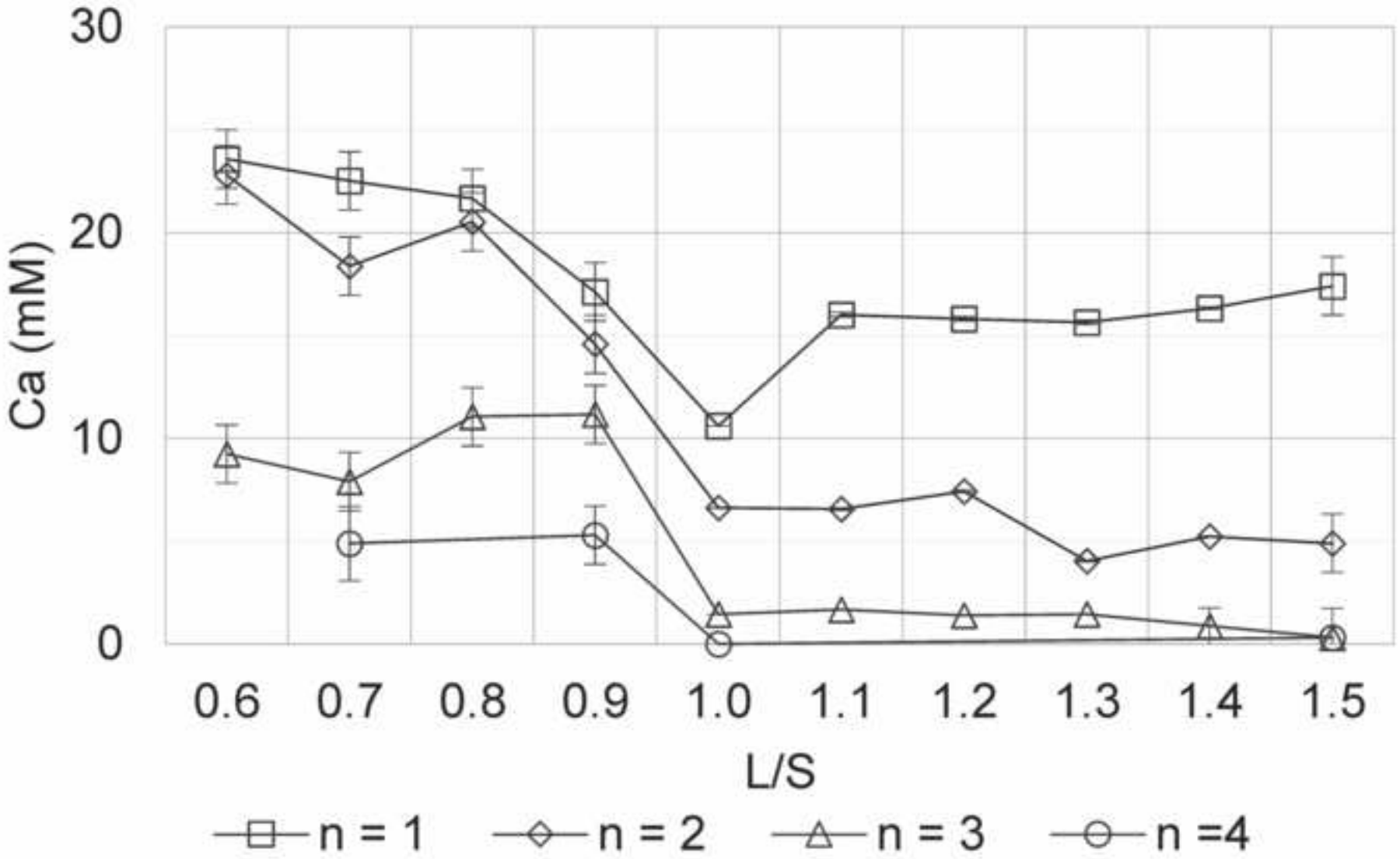

CarlaCC

CarlJS

JosephCA

EhsanJ